International Journal of
Molecular Sciences

MDPI

Article

Macrocyclic Diterpenoids from *Euphorbia peplus* Possessing Activity Towards Autophagic Flux

Lu Chen [1], Lulan Liu [1], Yingyao Li [2], Shipeng Guan [2], Lingling Fan [1], Xujie Qin [2], Yingtong Di [2], Lei Tang [1], Rongcan Luo [3,*] and Ying Yan [1,*]

1 State Key Laboratory of Functions and Applications of Medicinal Plants & College of Pharmacy, Guizhou Provincial Engineering Technology Research Center for Chemical Drug R&D, Guizhou Medical University, Guiyang 550014, China
2 State Key Laboratory of Phytochemistry and Plant Resources in West China, Kunming Institute of Botany, Chinese Academy of Sciences, Kunming 650201, China; diyt@mail.kib.ac.cn (Y.D.)
3 Gansu Key Laboratory of Biomonitoring and Bioremediation for Environmental Pollution, and Key Laboratory of Cell Activities and Stress Adaptations, Ministry of Education, School of Life Sciences, Lanzhou University, Lanzhou 730000, China
* Correspondence: luorc@lzu.edu.cn (R.L.); yanying@gmc.edu.cn (Y.Y.)

Abstract: Euphjatrophanes H–L (**1**–**5**), four new jatrophane-type and one new lathyrane-type diterpenoid, were isolated from *Euphorbia peplus*, along with eight known diterpenoids (**6**–**13**). Their structures were established on the basis of extensive spectroscopic analysis and X-ray crystallographic experiments. All compounds were subjected to bioactivity evaluation using flow cytometry in autophagic flux assays with HM mCherry-GFP-LC3 cells, the human microglia cells which stably expressed the tandem monomeric mCherry-GFP-tagged LC3. Compounds **1**–**3**, **5**–**10**, and **12** significantly increase autophagic flux, and compounds **1** and **12** displayed relatively high BBB permeability, with log*Pe* values of −4.853 and −5.017, respectively. These findings indicated that jatrophane diterpenoids could serve as a valuable source for innovative autophagy inducers.

Keywords: euphjatrophane; *Euphorbia peplus*; macrocyclic diterpenoid; autophagy; blood–brain barrier permeation

Academic Editor: Bruno Rizzuti

Received: 13 December 2024
Revised: 30 December 2024
Accepted: 31 December 2024
Published: 31 December 2024

Citation: Chen, L.; Liu, L.; Li, Y.; Guan, S.; Fan, L.; Qin, X.; Di, Y.; Tang, L.; Luo, R.; Yan, Y. Macrocyclic Diterpenoids from *Euphorbia peplus* Possessing Activity Towards Autophagic Flux. *Int. J. Mol. Sci.* **2025**, *26*, 299. https://doi.org/10.3390/ijms26010299

1. Introduction

Over the past decades, phytochemical research has always focused on the structurally diverse diterpenoids from the plants of the genus *Euphorbia*, resulting in the numerous diterpenoids featuring jatrophane, ingenane, pepluane, paraliane, and segetane scaffolds [1–9]. For instance, Resiniferatoxin, a diterpenoid of the daphnane type isolated from *E. resinifera*, is renowned for its ability to relieve neuropathic pain and is currently undergoing Phase I human clinical trials for the treatment of severe pain in cancer patients [10]. Euphodendroidin D, for example, is a jatrophane-type diterpenoid derived from *E. dendroides* that exhibits inhibitory effects on the transport activity of P-glycoprotein, an ABC transporter protein associated with multidrug resistance by lowering the intracellular drug concentration [11]. In 2012, the FDA approved ingenol 3-angelate, an ingenane-type diterpenoid obtained from *E. peplus*, for the treatment of actinic keratosis [12].

E. peplus Linn., a tiny annual weed originally from the Mediterranean coastline, was introduced to Yunnan province in China. Presently, it is found across the globe and has served as a traditional remedy for numerous years to address skin conditions, inflammatory disorders, asthma, diabetes, and various cancers [13]. Ingenane-type diterpenoids, specifically 20-deoxyingenol and its derivatives, have ever been reported by our research

group. These compounds exhibited the ability to stimulate lysosome biogenesis and inhibit amyloid plaque formation in the brains of APP/PS1 mice [14]. This finding indicates their promising potential for the therapy of Alzheimer's disease.

The subsequent phytochemical studies of the plants of the genus *Euphorbia* led to the isolation of several novel diterpenoids with significant bioactivities. Among them, jatrophane-type diterpenes could significantly activate the lysosomal–autophagy pathway, which suggested that the *Euphorbia* diterpenoids could potentially be an important source for novel anti-Alzheimer's disease (AD) drugs [15]. In our continuing efforts to uncover structurally novel diterpenes capable of inducing lysosomal biogenesis, four new jatrophane-type and one new lathyrane-type diterpenoid, named euphjatrophanes H–L (**1**–**5**), along with eight previously reported diterpenoids (**6**–**13**), were obtained from *E. peplus* (Figure 1). Their structures were elucidated using extensive NMR, X-ray crystallographic, and electronic circular dichroism (ECD) experiments. Moreover, compounds **1** and **12** displayed significant activity on autophagic flux and had relatively high BBB permeability. Herein, we reported the structural elucidation and biological evaluation of these compounds.

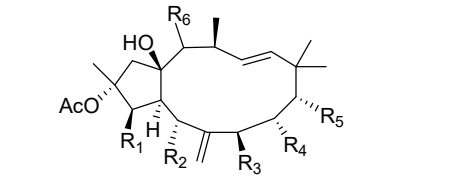

	R_1	R_2	R_3	R_4	R_5	R_6
1	OBz	OAc	OiBu	OH	OBz	β-OAc
3	OBz	OAc	OiBu	OH	ONic	β-OH
11	OAc	OiBu	OBz	OAc	OAc	β-OAc
12	OBz	OAc	OTig	OAc	OAc	α-OAc

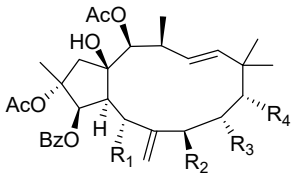

	R_1	R_2	R_3	R_4
2	OAc	OPr	OH	ONic
7	OAc	OiBu	OAc	ONic
8	OAc	OiBu	OH	ONic
9	OAc	OAc	OH	ONic
10	OAc	OPr	OAc	OAc

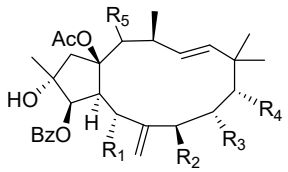

	R_1	R_2	R_3	R_4	R_5
4	OH	OiBu	OAc	ONic	O
6	OAc	OiBu	OAc	OAc	β-OAc

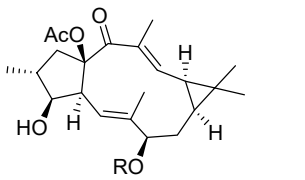

5 R = 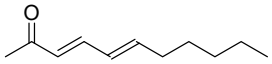

13 R = 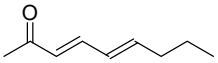

Figure 1. The chemical structures of compounds **1**–**13**.

2. Results

2.1. Structure Elucidation

Compound **1** was obtained as a colorless cube crystal. The identification of its molecular formula of $C_{44}H_{54}O_{14}$ was achieved based on its HRESIMS ion at m/z 829.3407 $[M + Na]^+$ (calculated for 829.3406), corresponding to 18 degrees of unsaturation (DOUs). Its ^1H and ^{13}C-DEPT NMR spectra indicated the presence of three acetyls [δ_H 2.01, 2.10, and 2.18 (each 3H, s); δ_C 20.5, 21.1, 22.4, 168.5, 170.5, and 170.8], two benzoyloxy groups [δ_H 7.42, 7.45, 7.55, and 7.58 (each 2H), 7.55, and 7.58 (each 1H); δ_C 128.4 × 2, 128.5 × 2, 129.7 × 2, 130.3 × 2, 129.0, 130.1, 133.1, 133.6, 164.8, and 167.2], and one isobutyryloxy group [δ_H 1.92 (m, 1H), 0.91, 0.41 (each 3H); δ_C 17.2, 19.1, 33.5, and 174.2]. Apart from these acyl groups, the ^{13}C NMR also showed twenty carbon signals, including four methyls (δ_C 23.2, 23.3, 23.6,

and 27.5), one sp^3 methylene (δ_C 50.0), eight sp^3 methines with six oxygenated (δ_C 37.5, 44.8, 68.2, 70.4, 71.9, 79.3, 80.5, and 86.4), three sp^3 non-proton-bearing carbons with two oxygenated (δ_C 40.4, 84.3, and 88.5), an exocyclic double bond [δ_H 4.45, and 4.83 (each, br s, 1H); δ_C 109.0, and 144.3], and a trans-disubstituted double bond [δ_H 6.15 (d, J = 16.0 Hz), and 5.66 (dd, J = 9.6, 16.0 Hz); δ_C 131.2, and 134.0] (Table 1). Further signals were detected in the ^{1}H NMR spectrum of **1** for the resonances of two exchangeable protons [δ_H 3.13, 3.48]. Among the 18 indices of hydrogen deficiency, 16 were attributed to 2 benzoyls, 3 acetyls, an isobutyryl, and 2 double bonds. The remaining two DOUs were assumed to be due to the presence of the bicyclic system of **1**. Therefore, it could be deduced to be a jatrophane polyester.

Table 1. ^{1}H (500 MHz) and ^{13}C (125 MHz) NMR data of compounds **1**−**3** in $CDCl_3$.

	1		**2**		**3**	
No.	δ_H (J in Hz)	δ_C	δ_H (J in Hz)	δ_C	δ_H (J in Hz)	δ_C
1	2.82, d (14.3)	50.0	2.83, overlap	49.7	2.68, overlap	50.7
	2.10, d (14.3)		2.06, overlap		2.02, overlap	
2		88.5		88.5		88.0
3	5.92, d (5.8)	80.5	5.94, d (5.6)	80.7	5.88, d (5.5)	81.1
4	3.66, dd (5.8, 3.5)	44.8	3.75, dd (5.6, 3.6)	44.9	3.48, dd (9.6, 4.8)	44.5
5	5.79, d (3.5)	71.9	5.80, d (3.6)	72	5.79, d (3.8)	71.9
6		144.3		143.8		144.5
7	5.35, s	68.2	5.35, s	68.7	5.39, s	68.2
8	4.12, d (11.2)	70.4	4.15, d (10.8)	70.2	4.17, d (10.2)	70.2
9	5.03, s	86.4	5.09, s	86.6	5.06, s	87.1
10		40.4		40.4		40.4
11	6.15, d (16.0)	134.0	6.16, d (15.9)	133.9	6.03, br s	132.5
12	5.66, dd (16.0, 9.6)	131.2	5.68, dd (16.0, 9.6)	131.6	6.02, br s	132.3
13	2.87, m	37.5	2.85, m	37.6	2.66, m	37.7
14	5.14, s	79.3	5.14, s	79.4	3.66, s	78.6
15		84.3		84.4		85.5
16	1.49, s	23.3	1.48, s	23.6	1.36, s	23.3
17	4.83, br s	109.0	4.78, br s	109.1	4.86, br s	109.1
	4.45, br s		4.46, br s		4.49, br s	
18	1.07, s	27.5	1.07, s	27.3	1.06, s	27.6
19	1.36, s	23.2	1.36, s	23.1	1.51, s	22.7
20	1.17, d (7.0)	23.6	1.18, d (7.0)	23.6	1.25, d (6.9)	24.5
OAc-2						
C=O		170.8		171.1		170.8
	2.18, s	22.4	2.21, s	22.5	2.19, s	22.5
OAc-5						
C=O		168.5		168.6		168.5
	2.01, s	21.1	2.10, s	20.6	1.99, s	20.9
OAc-14						
C=O		170.5		170.5		
	2.10, s	20.5	2.03, s	21.1		
OBz-3						
C=O		164.9		164.9		164.7
1′		129.0		130		130.0
2′,6′	8.05, d (8.2)	129.7	8.07, d (8.2)	129.7	8.06, d (8.2)	129.6
3′,5′	7.42, t (7.8)	128.4	7.42, t (7.8)	128.4	7.46, t (7.8)	128.5
4′	7.55, t (7.4)	133.1	7.56, t (7.4)	133.2	7.58, t (7.4)	133.2
OiBu/OPrp-7						
C=O		174.2		171.5		174.4
1″	1.92, m	33.5	1.92, m	27.1	1.97, m	33.6
2″	0.91, d (7.0)	19.1	1.65, m		0.48, d (6.8)	17.4
3″	0.41, d (6.8)	17.2	0.60, t (7.5)	8.2	0.94, d (7.0)	19.1
ONic/OBz-9						
C=O		167.2		165.7		165.9
1‴		130.1	9.30, d (1.4)	151.5	9.28, d (1.8)	151.5
2‴	8.09, d (8.2)	130.3		125		125.1
3‴	7.45, m	128.5	8.35, dt (8.0, 1.6)	137.4	8.35, dt (8.0, 4.8)	137.5
4‴	7.58, m	133.6	7.40, dd (8.0, 4.8)	123.3	7.41, dd (8.0, 4.8)	123.4
5‴			8.82, dd (4.9, 1.8)	154.1	8.82, dd (4.9, 1.7)	154.0
OH-8	3.13 d (11.2)					
OH-15	3.48, s		3.65, s		3.98, s	

Analyses of the 2D NMR data enable the assembly of the aforementioned functionalities and then establish the structure of **1**. Three structural fragments, namely C-3/C-4/C-5 (fragment A), C-7/C-8/C-9 (fragment B), and C-11/C-12/C-13(Me-20)/C-14 (fragment C), were deduced from the analysis of 1H-1H COSY and HSQC spectra (Figure 2). HMBC correlations from H-4 (δ_H 3.66) to C-14 (δ_C 79.3) and C-15 (δ_C 84.3), and H-14 (δ_H 5.14) to C-4 (δ_C 44.8) and C-15 (δ_C 84.3) suggested that fragments A and C were linked through C-15. Fragments B and C were inferred to be interconnected via gem-dimethyl and carbonyl groups, supported by HMBC correlations from H3-19 (δ_H 1.36)/H3-18 (δ_H 1.07) to C-9 (δ_C 86.4), C-10 (δ_C 40.4), and C-11 (δ_C 134.0); H-9 (δ_H 5.03) to C-10 (δ_C 40.4) and C-11 (δ_C 134.0). Cross peaks of H2-17 (δ_H 4.83, 4.45) to C-5 (δ_C 71.9), C-6 (δ_C 144.3), and C-7 (δ_C 68.2) in the HMBC spectrum indicated the connection between fragments A and B, and CH2-17 through the olefinic carbon C-6. In addition, The HMBC correlations from H2-1 (δ_H 2.82, 2.10) to C-4 (δ_C 44.8) and C-15 (δ_C 84.3), from Me-16 (δ_H 1.49) to C-1 (δ_C 50.0), C-2 (δ_C 88.5), and C-3 (δ_C 80.5) indicated the presence of a five-membered ring. Finally, cross peaks of H-2/the acetyl carbonyl (δ_C 170.8), H-3/the benzoyl carbonyl (δ_C 164.9), H-5/the acetyl carbonyl (δ_C 168.5), H-7/the isobutyryl carbonyl (δ_C 174.2), H-9/the benzoyl carbonyl (δ_C 167.2), H-14/the acetyl carbonyl (δ_C 170.5) in HMBC spectrum could be located the three acetoxy groups at C-2, C-5, and C-14, the two benzoyloxy groups at C-3, and C-9, and the isobutyryl group at C-7. The remaining two hydroxyls must be located at C-8, and C-15, respectively. Thus, the gross structures of **1** were established, as shown in Figure 2.

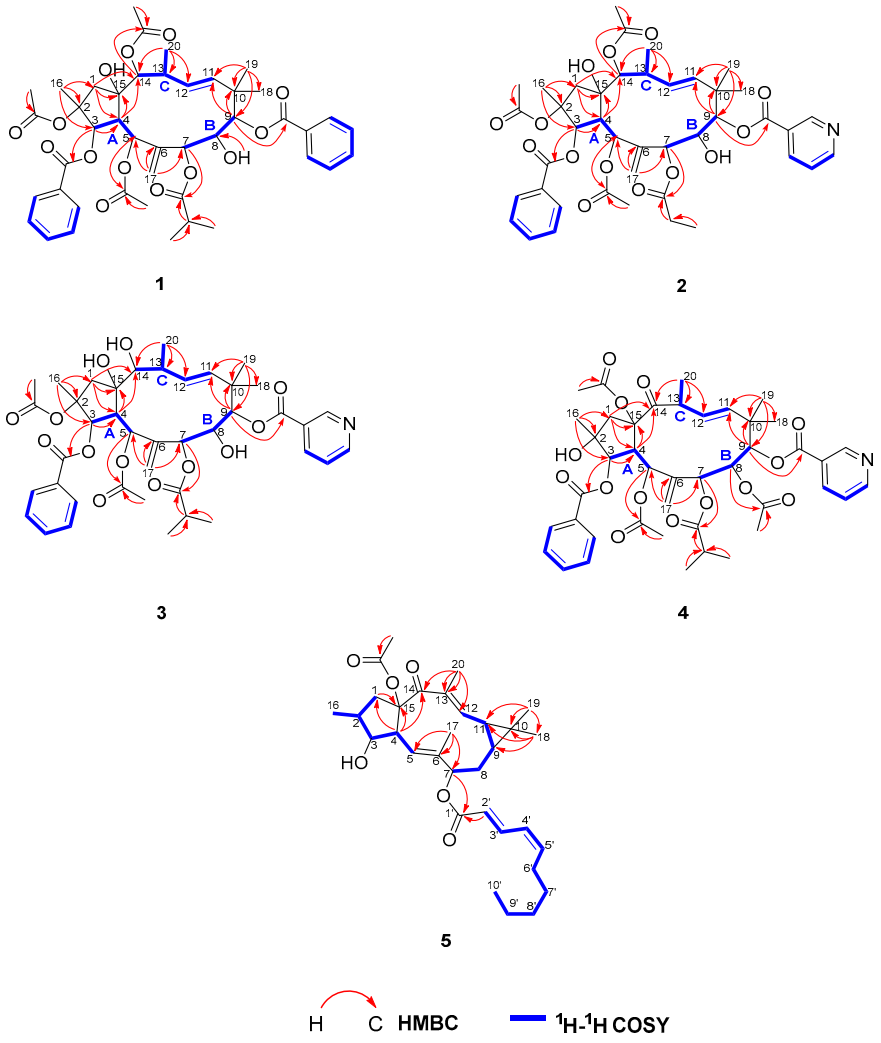

Figure 2. ^{1}H−^{1}H COSY correlations and key HMBC of compounds **1**–**5**.

The relative configuration of **1** was determined to be the same as that of the known compound, 2,5,14-triacetoxy-3-benzoyloxy-8,15-dihydroxy-7-isobutyroyloxy-9-nicotinoyloxyjatropha-6(17), 11E-diene [16], based on their similar ^{1}H and ^{13}C NMR data and ROESY correlations (Figure 3). A single-crystal X-ray diffraction by Cu Kα radiation [CCDC: 2408429, Flack parameter: 0.11(6)] allowed an unambiguous assignment of the absolute configuration for **1** as 2*R*,3*R*,4*S*,5*R*,7*S*,8*R*,9*S*,13*S*,14*S*,15*R* (Figure 4).

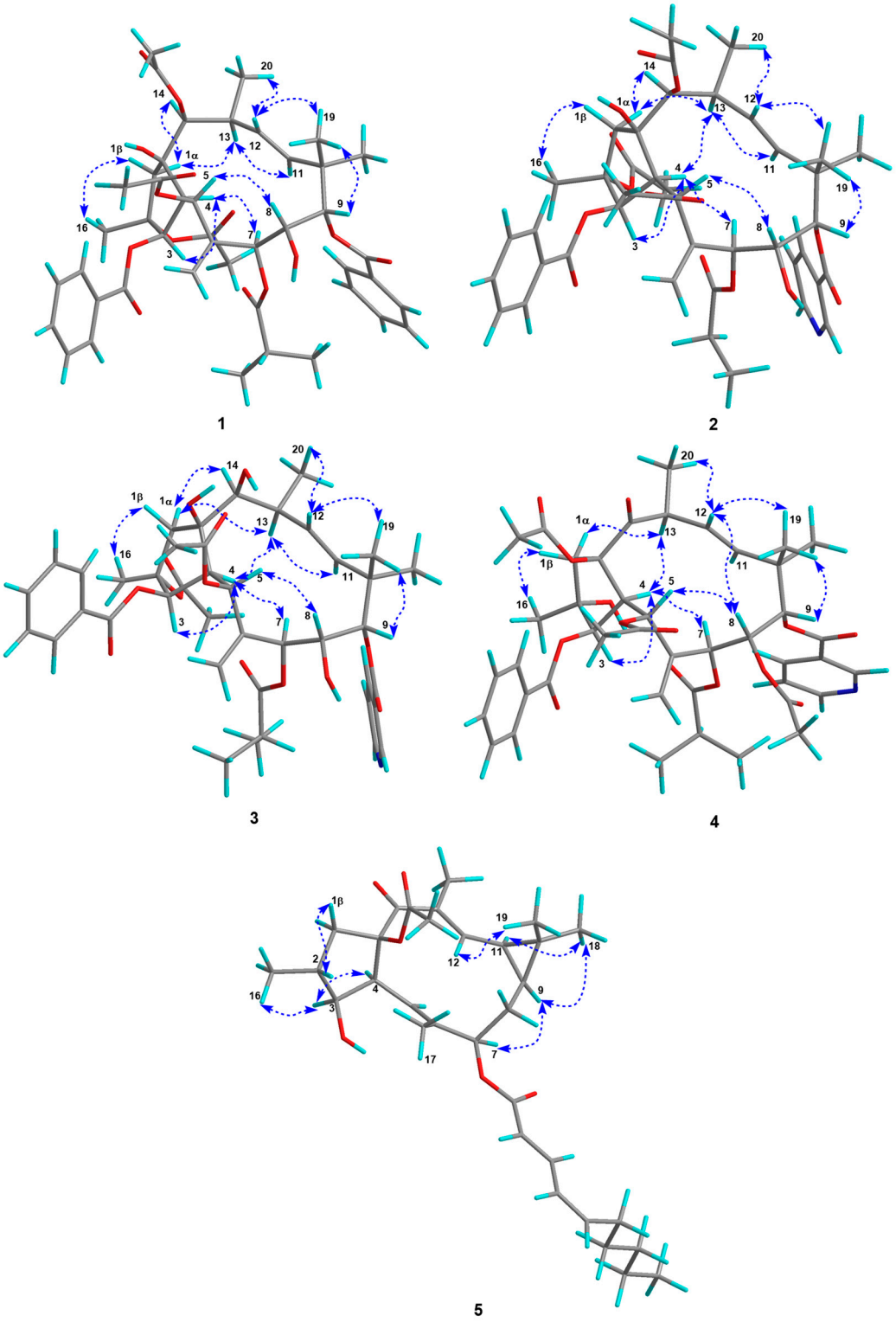

Figure 3. Selected ROESY correlations of compounds **1**–**5**.

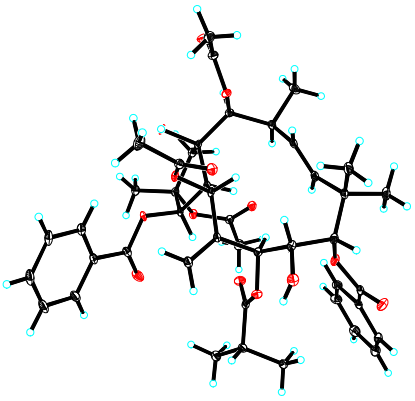

Figure 4. X-ray ORTEP drawing of euphjatrophane H (**1**).

Euphjatrophane I (**2**), a white powder, was assigned a molecular formula of $C_{42}H_{51}NO_{14}$, as deduced from its HRESIMS (*m*/*z* 794.3390 $[M + H]^+$, calculated for $C_{42}H_{52}NO_{14}$, 794.3382). The ^1H and ^{13}C NMR data (Table 1) of **2** showed a high similarity to euphjatrophane H (**1**), but one propionyloxy group (δ_H 1.92, 1.65, 0.60; δ_C 171.5, 27.1, 8.2) and one nicotinoyloxy group (δ_H 9.30, 8.82, 8.35, 7.40; δ_C 165.7, 154.1, 151.5, 137.4, 125.0, 123.3) occurred in compound **2** instead of the isobutyryloxy group and benzoyloxy group in the latter (Table 1). An extensive analysis of the HSQC, HMBC, and ^1H-^1H COSY spectra permitted a C-7 propionyloxy group and a C-9 nicotinoyloxy group in euphjatrophane I (**2**). In addition, the relative configuration of euphjatrophane B (**2**) was established as shown on the basis of the ROESY spectrum (Figure 3).

Compound **3** was obtained as a white powder, and the HRESIMS data showed an $[M + H]^+$ ion at *m*/*z* 766.3435 (calculated for $C_{41}H_{52}NO_{13}$, 766.3433), corresponding to the molecular formula $C_{41}H_{51}NO_{13}$. The 1D NMR data (Table 1) of **3** showed a high similarity to those of euphjatrophane H (**1**) with the exception of the absence of the resonances from one benzoyloxy group and the presence of one nicotinoyloxy group (δ_H 9.28, 8.82, 8.35, 7.41; δ_C 165.9, 154.0, 151.5, 137.5, 125.1, 123.4). The HMBC correlations from H-9 (δ_H 5.06) to the nicotinoyl's carbonyl (δ_C 165.9) revealed that the nicotinoyloxy group was located at C-9. On the grounds of the ROESY correlations analysis, the relative configuration of **3** was determined to be the same as that of euphjatrophane H (**1**). Specifically, the ROESY correlations of H-1α/OAc-2, H-3/H-4, H-4/H-7, H-4/H-13, H-7/H-11, and H-11/H_3-18, as well as H-5/H-8, H-8/H-12, H-8/H_3-19, and H-9/H_3-19, were observed.

Euphjatrophane K (**4**) was also obtained as an amorphous white solid and possessed the molecular formula $C_{41}H_{49}NO_{13}$, based on its HRESIMS ion at *m*/*z* 786.3112 $[M + Na]^+$ (calculated for $C_{41}H_{49}NO_{13}Na$, 786.3102). The ^1H and ^{13}C NMR data of euphjatrophane K (4) were closely related to those of the isolated euphopeplin A (**7**), except for one carbonyl group occurring in euphjatrophane K (**4**) instead of the acetoxy group at C-14 in euphopeplin A (Table 2), as evidenced by the crucial HMBC correlation from H_2-1/H-4/H_3-20 to the ketone carbonyl (δ_C 212.5) (Figure 2). The remaining relative configurations of euphjatrophane K (**4**) were the same as those of euphopeplin A (**7**) based on their similar 1D NMR shifts and ROESY data. Furthermore, the similar electronic circular dichroism (ECD) spectra of compounds **1**−**4** (Figure 5) indicated they shared the same absolute configuration.

Table 2. ^{1}H and ^{13}C NMR data of compounds **4** and **5**.

	4 [a]		**5** [b]	
No.	δ_H (*J* in Hz)	δ_C	δ_H (*J* in Hz)	δ_C
1	2.13, d (15.0)	50.0	2.61, dd (14.0, 10.2)	40.8
	3.21, d (15.0)		2.23, t (10.4)	
2		90.9	2.15, m	40.6
3	6.11, d (5.6)	79.7	3.83, dd (8.0, 4.8)	81.6
4	3.77, dd (5.8, 2.8)	48.9	2.62, dd (13.8, 3.6)	48.9
5	5.57, s	69.7	6.05, d (13.0)	121.2
6		146.3		143.4
7	4.36, s	69.8	4.89, dd (13.8, 3.6)	76.8
8	5.08, s	70.7	2.41, dt (16.4, 4.0)	33.2
9	5.14, s	82.2	1.83, m	30.2
10		41.7	1.14, m	24.3
11	6.24, d (15.8)	137.2	1.29, overlap	29.1
12	5.60, dd (15.8, 10.2)	132.1	6.58, d (13.6)	145.3
13	4.12, dd (9.6, 6.6)	45.4		133.1
14		212.5		194.7
15		90.9		96.3
16	1.52, s	22.1		18.3
17	4.96, br s	111.5	1.08, d (8.2)	18.8
	4.88, br s		1.56, s	
18	1.26, s	22.5	1.19, s	29.0
19	1.03, s	26	1.09, s	16.2
20	1.29, d (6.6)	19.2	1.84, s	12.2
OAc-8				
C=O		170.3		
	1.41, s	19.9		
OAc-15				
C=O		172		169.7
	2.30, s	22	2.04, s	21.7
OBz-3				
C=O		166.4		
1′		130.8		
2′,6′	8.08, d (8.2)	130.5		
3′,5′	7.47, t (7.8)	129.1		
4′	7.61, t (7.4)	133.9		
OiBu-7				
C=O		177.0		
1″	2.56, m	34.6		
2″	1.10, d (7.0)	18.9		
3″	1.14, d (6.8)	18.7		
ONic-9				
C=O		164.5		
1‴	9.22, d (2.2)	151.2		
2‴		126.4		
3‴	8.49, d (8.4)	138.8		
4‴	7.65, dd (8.0, 4.8)	124.9		
5‴	8.86, dd (5.0, 1.6)	154.4		
OR-7				
1⁗				166.9
2⁗			5.89, overlap	120.8
3⁗			7,63, dd (18.4, 14.0)	140.2
4⁗			6.12, t (13.4)	126.3
5⁗			5.88, overlap	142.3
6⁗			1.48, dd (13.8, 9.6)	29.1
			1.42, t (8.8)	
7⁗			2.26, m	28.3
8⁗			1.28, overlap	31.4
9⁗			1.30, overlap	22.5
10⁗			0.88, t (7.8)	14.0

[a] Data measured at 400 MHz and 100 MHz in CD_3OD; [b] data measured at 600 MHz and 150 MHz in $CDCl_3$.

Euphjatrophane L (**5**) was isolated as a yellow oil, and its molecular formula was deduced as $C_{32}H_{46}O_6$ by the observed HRESIMS ion at *m*/*z* 527.3372 $[M + H]^+$, calculated for $C_{32}H_{47}O_6$, 527.3367, indicating 10 DOUs. The ^{1}H and ^{13}C NMR data (Table 2) of **5** indicated the presence of one acetyl (δ_H 2.04; δ_C 169.7, 21.7), one (2*E*,4*Z*)-deca-2,4-dienoyl (δ_H 6.58; δ_C 194.7,145.3, 133.1), one exocyclic double bond, and one trisubstituted α,β-

unsaturated ketone moiety (δ_H 7.63, 6.12, 5.89, 5.88, 2.26, 1.48, 1.42, 1.30, 1.28, 0.88; δ_C 166.9, 142.3, 140.2, 126.3, 120.8, 31.4, 29.1, 28.3, 22.5, 14.0). Among the ten DOUs, seven were attributed to one acetyl, one (2*E*,4*Z*)-deca-2,4-dienoyl, two double bonds, and one ketone carbonyl. The remaining three DOUs were assumed to be due to the presence of the tricyclic system of **1**. Moreover, resonances [δ_H 1.14 (H-9), 1.29 (H-11), 1.19 (H_3-18), 1.09 (H_3-19), and δ_C 24.3 (C-10), as well as two tertiary methyl groups at δ_H 1.56 (H_3-17) and 1.84 (H_3-20)], were observed which are characteristic signals for a gem-dimethyl cyclopropane moiety. Therefore, it could be deduced to be a lathyrane-type polyester with a 5/11/3-tricyclinc skeleton (Table 2).

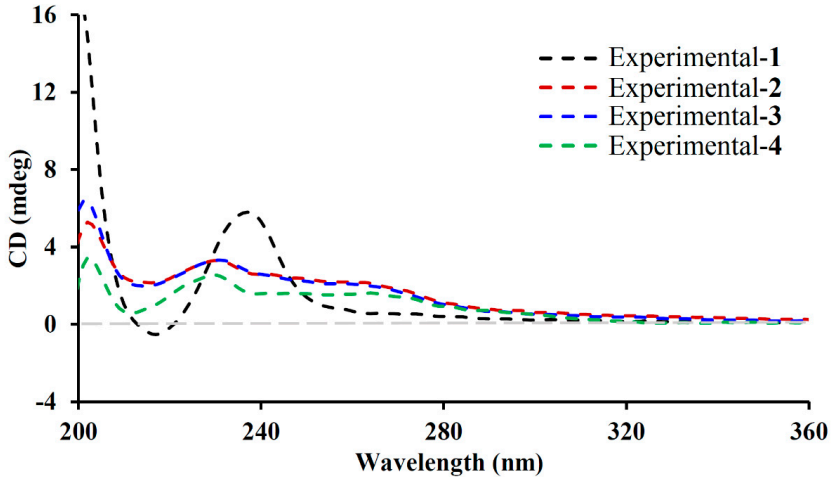

Figure 5. Measured ECD spectra of compounds **1**–**4**.

A comparison of the ^{1}H and ^{13}C NMR spectra of compound **5** with euphohelioscopin B suggested that they have the same lathyrane ring system [17], except for one (2*E*,4*Z*)-2,4-dienoyloxy group at C-7 occurring in compound **5** instead of the 4,5-dihydroxy-2*E*-octenoyloxy moiety in euphohelioscopin B. This finding was further supported by the HMBC cross-peak from H-7 (δ_H 4.89) to the carbonyl carbon (δ_C 166.9). In addition, the relative configuration at the remaining chiral centers of euphjatrophane L (**5**) would be analogous to those of the latter on the basis of ^{13}C NMR shifts and NOE data.

Furthermore, nine previously identified diterpenoids, named euphpepluones G (**6**) [15], euphopeplin A (**7**) [6], 2,5,14-triacetoxy-3-benzoyloxy-8,15-dihydroxy-7-isobutyroyloxy-9-nicotinoyloxyjatropha-6(17),11E-diene (**8**) [16], 2, 5,7,14-tetraacetoxy-3-benzoyloxy-8,15-dihydroxy9-nicotinoyloxyjatropha-6(17),11E-diene (**9**) [16], 2α,5α,8α,9α,14β-Pentaacetoxy-3β-benzoyloxy-7-propionyloxyjatropha-6(17),11E-dien-15β-ol (**10**) [18], pepluanin C (**11**) [19], euphpepluone F (**12**) [20], and Euphohelioscopin A (**13**) [17], were characterized through a comparative analysis of their MS and NMR data with the established literature values.

2.2. X-Ray Diffraction Data Analysis

A suitable crystal of **1** was selected and recorded on a Bruker APEX DUO diffractometer equipped with an APEX II CCD using Cu Kα radiation. Cell refinement and data reduction were performed with Bruker SAINT Software Version 6.45. The structures were solved by direct methods using SHELXS-97, and refinements were performed with SHELXL-97 using full-matrix least-squares, with anisotropic displacement parameters for all the non-hydrogen atoms; hydrogen atoms were placed in calculated positions and refined using a riding model. Molecular graphics were computed with PLATON. The crystallographic data were deposited at the Cambridge Crystallographic Data Center with the deposition number CCDC 2408429.

Crystal data for **1**: $C_{44}H_{54}O_{14}\cdot H_2O$, M = 824.88, a = 10.9602(5) Å, b = 15.0409(7) Å, c = 25.4717(11) Å, α = 90°, β = 90°, γ = 90°, V = 4199.0(3) Å3, T = 100.(2) K, space group P212121, Z = 4, μ(Cu Kα) = 0.815 mm^{-1}, 39,527 reflections measured, and 7952 independent reflections (*Rint* = 0.1415). The final R_1 values were 0.0531 ($I > 2\sigma(I)$). The final $wR(F^2)$ values were 0.1207 ($I > 2\sigma(I)$). The final R_1 values were 0.0681 (all data). The final $wR(F^2)$ values were 0.1252 (all data). The goodness of fit on F^2 was 1.119, and the Flack parameter = 0.11(6).

2.3. Bioactivity of the Compounds Towards Autophagic Flux

The bioactivity of all the compounds towards autophagic flux was evaluated using HM mCherry-GFP-LC3 cells by flow cytometry (Figure 6). It is noteworthy that our findings revealed that compounds **1**−**3**, **5**−**10**, and **12** significantly increased autophagic flux, particularly for compounds **1** and **12**, which exhibited the most promising activity in this regard. In contrast, compounds **2**, **4**, **11**, and **13** did not significantly influence autophagic flux and, in fact, exhibited no significant effect on autophagic flux. The structure–activity relationships of these jatrophane diterpenoids and lathyrane diterpenoids were briefly analyzed. Compound **12** exhibited significantly activated autophagic flux compared to compounds **2**, **4**, and **11**, which indicated that ring A, containing ketone functionality and an acetyl group at C-14 in *R* configuration, completely lost activity. When considering **1**, **2**, **4**, and **11** specifically, compound **1** showed a relatively more potent activated autophagic flux, suggesting that the presence of both an isobutyryl group at C-7 and a benzoyl group at C-9 might contribute to the resultant activated autophagic flux. A comparison of the activated autophagic flux activity of **6** with those of **7** indicated that the presence of an acetyl group at C-2 may contribute to the higher activity. The activated autophagic flux of **8** and **9** suggested that the isobutyryl group at C-7 might cause a decrease in activity. Regarding **5** and **13** specifically, compound **5** demonstrated relatively more potent activated autophagic flux than **13**, implying that the presence of a (2*E*,4*Z*)-2,4-decadienoic acid ester group at C-7 might contribute to the observed activated activities.

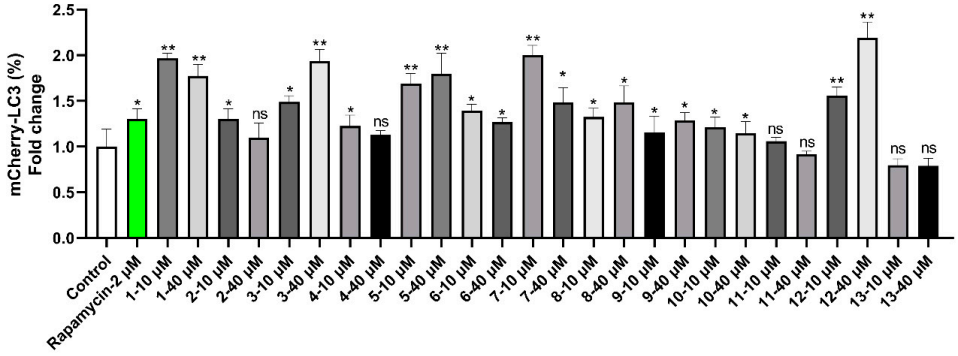

Figure 6. Flow cytometry analysis shows the bioactivity of compounds **1**–**13** towards autophagic flux. Rapamycin (2 μM) was used as the control. The results are presented as the mean ± SD (n = 3): * $p < 0.05$, ** $p < 0.01$, ns, not significant, compared to control.

2.4. Blood–Brain Barrier (BBB) Permeation

In the development of effective therapeutic drug candidates for neurodegenerative diseases, assessing the permeability of molecules across the blood–brain barrier (BBB) plays an important role. We employed a parallel artificial membrane permeability assay tailored for the blood–brain barrier (PAMPA-BBB) to ascertain the brain penetration capability of compounds **1** and **12**, utilizing three commercially available drugs, carbamazepine, propranolol, and furosemide, as references. The result of the PAMPA-BBB assay (Table 3) indicates that compounds **1** and **12** have excellent BBB permeability, with log*Pe* values of −4.853 and −5.017, respectively.

Table 3. Permeability (log*Pe*) in the PAMPA-BBB assay for commercial drugs and compounds **1** and **12** with prediction of their penetration to the CNS.

Compounds	log*Pe*	Prediction	Compounds	log*Pe*	Prediction
Carbamazepine	−3.782 ± 0.816	CNS ++	**1**	−4.853 ± 0.076	CNS ++
Propranolol	−3.593 ± 0.089	CNS ++	**12**	−5.017 ± 0.122	CNS +
Furosemide	−6.367 ± 0.562	CNS −			

− is not detected in acceptor or log*Pe* < −6.0, + is log*Pe* > −6.0, ++ is log*Pe* > −5.0.

3. Discussion

Previous research results from our research group indicate that jatrophane diterpenes can activate autophagy and induce lysosomal biogenesis. In vivo studies have shown that these compounds can clear amyloid-β in the brains of mice, suggesting that these compounds are an important source for the treatments for neurodegenerative diseases [14,15]. To identify more Euphorbia diterpenoids, which could induce and activate autophagy and lysosomal biogenesis from the plants of the genus *Euphorbia*, we studied the chemical composition of *E. peplus*. Jatrophane diterpenoids predominantly exist as polyesters, sharing a key 5/12 bicyclic pentadecane framework. Additional structural variations involve a range of oxygenated substituents and stereochemical attributes within their inherently flexible 5/12 bicyclic scaffold. Consequently, X-ray single crystal diffraction, particularly utilizing Cu Kα radiation, is frequently employed in structural analysis to precisely delineate their structures. Notably, the absolute configuration of compound **1** was unequivocally established through single-crystal X-ray diffraction analysis. Furthermore, the comparison of electronic circular dichroism (ECD) spectra for compounds **1**–**4** suggests they had the same absolute configuration.

Autophagy represents a conserved intracellular degradation pathway whereby unwanted or damaged organelles and misfolded proteins are delivered to lysosomes for breakdown. Given the pivotal role of autophagy defects in the pathogenesis of AD, the upregulation of autophagy has been proposed as a potential strategy for the prevention of this disease. The present study was designed to test the effect of compounds **1** and **12** on autophagy. The evaluation of small molecule permeability through the blood–brain barrier (BBB) is crucial for the development of effective drugs targeting neurodegenerative diseases. To investigate the ability of these jatrophane diterpenoids to penetrate the blood–brain barrier, a future study will be conducted to test the ability of compounds **1** and **12** to activate autophagy in vivo and in vitro in order to treat Alzheimer's disease. The present study also measured the brain penetration capability of compounds **1** and **12** using a tailored assay for the blood–brain barrier (PAMPA-BBB), which will provide a theoretical basis for conducting subsequent animal experiments.

In conclusion, four new jatrophane-type and one new lathyrane-type diterpenoid were isolated from the plants of *Euphorbia peplus*, along with eight known diterpenoids. The structures of these diterpenoids were elucidated through comprehensive NMR investigations, HRESIMS, and single-crystal X-ray diffraction analyses. Notably, Compounds **1**–**3**, **5**–**10**, and **12** significantly increase autophagic flux, and **1** and **12** exhibited the most promising activity in this regard. Moreover, PAMPA-BBB assays indicated that compounds **1** and **12** had the ability to penetrate the blood–brain barrier (BBB) through the process of transcellular passive diffusion. This study enriched the structural diversity of diterpenes and provided promising target molecules for the treatment of neurodegenerative diseases.

4. Materials and Methods

4.1. General Experimental Procedures

Optical rotations were measured on a Jasco P-1020 polarimeter (Jasco, Tokyo, Japan). UV spectra were obtained using a Shimadzu UV-2401A (Shanghai, China). IR spectra were recorded on a Bruker Tensor-27 infrared spectrophotometer with KBr disks. NMR spectra were collected on a Bruker Avance III 600 spectrometer (Bruker, Karlsruhe, Germany) using TMS as an internal standard. Waters Autospec Premier P776 mass spectrometers (Waters, Milford, MA, USA) were employed for HRESIMS measurements. Semipreparative HPLC was performed on an Agilent 1200 liquid chromatograph (Aglient, Santa Clara, CA, USA) with a Waters X-Bridge C18 (4.6 × 250 mm) column. Fractions were monitored by thin-layer chromatography (TLC, $HSGF_{254}$, Yantai Jiangyou silica Gel Development Co., Ltd., Yantai, China) and visualized by spraying with a Vanillin chromogenic agent (Chongqi, China). For column chromatography (CC), silica gel (90–150 μm, Qingdao Marine Chemical Ltd., Qingdao, China), Sephadex LH-20 gel (40–70 μm, Amersham Pharmacia Biotech AB, Uppsala, Sweden), and Lichroprep RP-C18 gel (40–63 μm, Merck, Darmstadt, Germany) were utilized. TLC spots were visualized under UV light and by dipping into 5% H_2SO_4 in EtOH, followed by heating.

4.2. Plant Material

The whole plants of *E. peplus*, identified by Prof. Shi-Jun Hu (Kunming Institute of Botany, Chinese Academy of Sciences), were collected in June 2022 from Guiyang, Guizhou Province, China. A voucher specimen (NODJ 20220713) has been deposited at the Laboratory of Guizhou Medical University.

4.3. Extraction and Isolation

The air-dried and powdered plant material (50.0 kg) was extracted with MeOH (3 × 40 L) under reflux three times (4, 3, and 3 h), respectively. The combined MeOH extracts were concentrated under a vacuum to obtain the crude residue (5.32 kg), which was suspended in water and then partitioned with EtOAc. The EtOAc portion (1728 g) was applied to a silica gel column using PE–EtOAc (50:1→5:1, v/v) and CH_2Cl_2–MeOH (20:1→1:1, v/v) to obtain seven fractions (Fr. 1–Fr. 6). Fr. 3 (163 g) was then separated over a MCI-gel column (MeOH–H_2O, 5:5→10:0, v/v) to obtain five fractions (Fr. 3A–Fr. 3E). Fr. 3D (49 g) was chromatographed over a C18 silica gel column, eluted with a gradient of MeOH–H_2O (6:4→10:0, v/v) to afford five subfractions (Fr. 3A1–Fr. 3A5). Fr. 3A3 (3.2 g) was applied to Sephadex LH-20 (MeOH) and semipreparative HPLC (70% MeOH in water) to obtain **6** (12.4 mg, t_R = 20.4 min) and **3** (14.2 mg, t_R = 25.6 min). Fr. 3A4 (2.9 g) was purified by silica gel column ($CHCl_2$–MeOH, 15:1, v/v) and then Sephadex LH-20 (MeOH) to **1** (9.5 mg), **9** (12.7 mg), and **11** (16.2 mg). Compounds **4** (10.5 mg) and **12** (13.1 mg) were obtained from Fr. 3A5 (2.5 g) by a silica gel column eluted with $CHCl_2$–MeOH (15:1, v/v) and Sephadex LH-20 (MeOH). Fr. 3E (37 g) was chromatographed on a C18 silica gel column eluted with a gradient of MeOH–H_2O (6:4→10:0, v/v) to afford four subfractions (Fr. 3E1–Fr. 3E4). Fr. 3E2 (1.2 g) was applied to Sephadex LH-20 (MeOH) and semipreparative HPLC (73% MeOH in water) to obtain **5** (9.7 mg, t_R = 23.4 min) and **13** (11.5 mg, t_R = 26.5 min). Fr. 3E3 (1.5 g) was purified by silica gel column ($CHCl_2$–MeOH, 10:1, v/v) and then Sephadex LH-20 (MeOH) to **7** (14.0 mg) and Fr. 3E3a. Fr. 3E3a (67 mg) was purified by semi-preparative HPLC (67% MeOH in water) to obtain **10** (10.9 mg, t_R = 22.0 min) and **12** (8.7 mg, t_R = 24.7 min). Fr. 3E4 (1.3 g) was applied to Sephadex LH-20 (MeOH) to yield **8** (19.8 mg).

Euphjatrophane H (**1**)

Colorless cube crystal (MeOH), mp 168.6–169.8 °C; $[\alpha]_D^{24}$ +122.4 (c 0.1, MeOH); UV (MeOH) λ_{max} (log ε) 195 (5.05); CD (MeOH) λ(Δε) 195 (−5.51), 200 (41.46), 216 (1.29), 237 (14.00); IR (KBr) ν_{max} 3589, 2972, 1729, 1601, 1451, 1376, 1234, 1112, 1024 cm^{-1}; ^1H and ^{13}C NMR data, see Table 1; HRESIMS *m*/*z* 829.3407 $[M + Na]^+$ (calculated for $C_{44}H_{54}O_{14}Na$, 829.3406).

Euphjatrophane I (**2**)

White amorphous powder; $[\alpha]_D^{24}$ +73.3 (c 0.132, MeOH); UV (MeOH) λ_{max} (log ε) 195 (4.80); CD (MeOH) λ(Δε) 195 (0.56), 202 (9.65), 215 (3.90), 230 (3.30); IR (KBr) ν_{max} 3443, 2970, 1728, 1591, 1374, 1276, 1235, 1114, 1024 cm^{-1}; ^1H and ^{13}C NMR data, see Table 1; HRESIMS *m*/*z* 794.3390 $[M + H]^+$ (calculated for $C_{42}H_{52}NO_{14}$, 794.3382).

Euphjatrophane J (**3**)

White amorphous powder; $[\alpha]_D^{24}$ +68.3 (c 0.12, MeOH); UV (MeOH) λ_{max} (log ε) 195 (4.86); CD (MeOH) λ(Δε) 195 (6.16), 201 (24.52), 214 (3.81), 230 (6.43); IR (KBr) ν_{max} 3425, 2928, 1727, 1660, 1373, 1278, 1115, 1068, 1024 cm^{-1}; ^1H and ^{13}C NMR ($CDCl_3$) data, see Table 1; HRESIMS *m*/*z* 766.3435 $[M + H]^+$ (calculated for $C_{41}H_{52}NO_{13}$, 766.3433).

Euphjatrophane K (**4**)

White amorphous powder; $[\alpha]_D^{24}$ +163.1 (c 0.2, MeOH); UV (MeOH) λ_{max} (log ε) 195 (4.79); CD (MeOH) λ(Δε) 195 (−12.57), 202 (7.20), 209 (1.45), 229 (5.22); IR (KBr) ν_{max} 3437, 2975, 1732, 1592, 1424, 1372, 1276, 1112, 1037 cm^{-1}; ^1H and ^{13}C NMR (CD_3OD) data, see Table 2; HRESIMS *m*/*z* 786.3112 $[M + Na]^+$ (calculated for $C_{41}H_{49}NO_{13}Na$, 786.3102).

Euphjatrophane L (**5**)

Yellow oil; $[\alpha]_D^{24}$ +80.1 (c 0.15, MeOH); UV (MeOH) λ_{max} (log ε) 204 (4.31), 272 (4.39); CD (MeOH) λ(Δε) 195 (46.25), 232 (−27.66), 272 (32.14); IR (KBr) ν_{max} 3438, 2928, 1740, 1622, 1373, 1266, 1064, 1006, 938 cm^{-1}; ^1H and ^{13}C NMR ($CDCl_3$) data, see Table 2; HRESIMS *m*/*z* 527.3372 $[M + H]^+$ (calculated for $C_{32}H_{47}O_6$, 527.3367).

4.4. Flow Cytometry Analysis

HM mCherry-GFP-LC3 cells, which stably express a triple fusion protein (red fluorescent protein (mCherry), green fluorescent protein (GFP), and the autophagy marker LC3, were created in our previous studies [14,15]. This triple-fusion protein is capable of directly reflecting the strength of autophagy flux. In the absence of autophagy, these cells exhibit yellow fluorescence due to the co-expression of red mCherry and green GFP. When autophagy is active, the process of autophagy leads to the fusion of autophagosomes and lysosomes, resulting in the formation of autolysosomes. The subsequent quenching of the acidic lysosomal environment causes the fluorescence of acid-sensitive GFP to be reduced, while mCherry remains unaffected. Consequently, the autolysosomes manifest red fluorescence. Consequently, the red fluorescence observed in the cells can be used as a marker for the formation of autolysosomes. The extent of red fluorescence can be used as an indicator of the efficiency of the flux from the autophagosome to the autolysosome [21]. The bioactivity of all compounds on autophagic flux was evaluated using HM mCherry-GFP-LC3 cells by flow cytometry [15]. In summary, the HM mCherryGFP-LC3 cells were cultured in 12-well plates for 24 h in DMEM (Dulbecco's modified Eagle medium) supplemented with 10% fetal bovine serum (Gibco-BRL, 10099–141, Gaithersburg, MD, USA) in a 37 °C incubator with 5% CO_2 at 95% humidity. Subsequently, the compounds were introduced directly to the culture medium, resulting in final concentrations of 10 μM and 40 μM. Rapamycin was used as a positive control. Twenty-four hours following the administration of the treatment,

the cells were harvested and fixed using 4% paraformaldehyde (PFA). This was followed by a flow cytometry test, which was conducted in order to determine whether autophagic flux had been altered. The data were analyzed using the FlowJo software v10 (BD Biosciences, Franklin Lakes, NJ, USA).

4.5. PAMPA-BBB Assay

We used the parallel artificial membrane permeability assay for BBB (PAMPA-BBB) to determine the brain permeability of compounds **1** and **12** [22]. The compounds **1** and **12** were prepared with methyl alcohol at the concentration of 4 mg/mL. These were diluted with PBS (Phosphate Buffer Saline; pH = 7.4) to obtain the donor solutions 100 μg/mL PAMPA "sandwich", consisting of a donor 96-well microliter plate and matching filter plate coated with 5 μL of 2% lecithin/dodecane. Compounds **1** and **12** were added to the wells (150 μL/well) of the pre-coated filter, and PBS was added to the wells (300 μL/well) of the receiver plate. The filter plate was coupled with the receiver plate, and the plate couple was incubated in the thermostat at 37 °C for 16 h. After incubation, the plates were separated, and the samples from each well of both the filter plate and the receiver plate were sucked out and analyzed by HPLC. See Supplementary Materials (Figures S1–S74).

4.6. Statistical Analysis

Data analyses were carried out by using GraphPad Prism 8 (GraphPad Software, Inc., La Jolla, CA, USA). The one-way ANOVA (analysis of variance) was performed using Dunnett's post hoc test for comparison between the treated group and control group, and the values were expressed as mean ± standard deviation (SD). It is considered to be statistically significant if p-value < 0.05; *, $p < 0.05$; **, $p < 0.01$; ***, $p < 0.001$.

Supplementary Materials: The supporting information can be downloaded at https://www.mdpi.com/article/10.3390/ijms26010299/s1.

Author Contributions: Y.Y., L.T. and R.L. designed experiments for this study. Y.Y., L.C. and L.L. isolated and characterized the compounds. R.L. and L.F. performed the bioactivity experiments. Y.L. and S.G. prepared crude extraction. Y.Y. prepared the manuscript. Y.D., X.Q. and R.L. revised the manuscript. All authors have read and agreed to the published version of the manuscript.

Funding: The work was supported financially by the National Natural Science Foundation of China (No. 82360687, 82471445, and 32170988), Guizhou Provincial Science and Technology Project (Grant No. ZK[2022]393), Guizhou High-level Innovative Talents Supporting Program (GCC [2023]002).

Institutional Review Board Statement: Not applicable.

Informed Consent Statement: Not applicable.

Data Availability Statement: The data underlying this study are available in the published article and its online Supplementary Materials.

Acknowledgments: We thank the analytical group of the Key Laboratory of Phytochemistry and Natural Medicines, Kunming Institute of Botany, and the Chinese Academy of Sciences for all spectroscopic analyses.

Conflicts of Interest: The authors declare no competing financial interests.

References

1. Rizk, A.M.; Hammouda, F.M.; Elmissiry, M.M.; Radwan, H.M.; Evans, F.J. Biologically active diterpene esters from *Euphorbia Peplus*. *Phytochemistry* **1985**, *24*, 1605–1606. [CrossRef]
2. Hohmann, J.; Günther, G.; Vasas, A.; Kálmán, A.; Argay, G. Isolation and structure revision of pepluane diterpenoids from *Euphorbia Peplus*. *J. Nat. Prod.* **1999**, *62*, 107–109. [CrossRef] [PubMed]

3. Hohmann, J.; Vasas, A.; GuÈnther, G.; Dombi, G.; Blazso, G.; Falkay, G.; MaÂthe, I.; Jerkovich, G. Jatrophane diterpenoids from *Euphorbia peplus*. *Phytochemistry* **1999**, *51*, 673–677. [CrossRef] [PubMed]
4. Hohmann, J.; Evanics, F.; Berta, L.; Bartok, T. Diterpenoids from *Euphorbia peplus*. *Planta Med.* **2000**, *66*, 291–294. [CrossRef]
5. Song, Z.Q.; Mu, S.Z.; Di, Y.T.; Hao, X.J. A new jatrophane diterpenoid from *Euphorbia peplus*. *Chin. J. Nat. Med.* **2009**, *7*, 81–83. [CrossRef]
6. Wan, L.S.; Chu, R.; Peng, X.R.; Zhu, G.L.; Yu, M.Y.; Li, L.; Zhou, L.; Lu, S.Y.; Dong, J.R.; Zhang, Z.R.; et al. Pepluane and paraliane diterpenoids from *Euphorbia peplus* with potential anti-inflammatory activity. *J. Nat. Prod.* **2016**, *79*, 1628–1634. [CrossRef]
7. Wan, L.S.; Nian, Y.; Ye, C.J.; Shao, L.D.; Peng, X.R.; Geng, C.A.; Zuo, Z.L.; Li, X.N.; Yang, J.; Zhou, M.; et al. Three minor diterpenoids with three carbon skeletons from *Euphorbia peplus*. *Org. Lett.* **2016**, *18*, 2166–2169. [CrossRef]
8. Hua, J.; Liu, Y.; Xiao, C.J.; Jing, S.X.; Luo, S.H.; Li, S.H. Chemical profile and defensive function of the latex of *Euphorbia peplus*. *Phytochemistry* **2017**, *136*, 56–64. [CrossRef]
9. Wan, L.S.; Nian, Y.; Peng, X.R.; Shao, L.D.; Li, X.N.; Yang, J.; Zhou, M.; Qiu, M.H. Pepluanols C–D, two diterpenoids with two skeletons from *Euphorbia peplus*. *Org. Lett.* **2018**, *20*, 3074–3078. [CrossRef]
10. Heiss, J.; Iadarola, M.; Cantor, F.; Oughourli, A.; Smith, R.; Mannes, A. (364) A phase I study of the intrathecal administration of resiniferatoxin for treating severe refractory pain associated with advanced cancer. *J. Pain* **2014**, *15*, S67. [CrossRef]
11. Corea, G.; Fattorusso, E.; Lanzotti, V.; Taglialatela-Scafati, O.; Appendino, G.; Ballero, M.; Simon, P.N.; Dumontet, C.; Di Pietro, A. Jatrophane diterpenes as P-glycoprotein inhibitors. First insights of structure-activity relationships and discovery of a new, powerful lead. *J. Med. Chem.* **2003**, *46*, 3395–3402. [CrossRef] [PubMed]
12. Berman, B. New developments in the treatment of actinic keratosis: Focus on ingenol mebutate gel. *Clin. Cosmet. Investig. Dermatol.* **2012**, *20*, 111–122. [CrossRef] [PubMed]
13. Ernst, M.; Grace, O.M.; Saslis-Lagoudakis, C.H.; Nilsson, N.; Simonsen, H.T.; Rønsted, N. Global medicinal uses of *Euphorbia* L. (Euphorbiaceae). *J. Ethnopharmacol.* **2015**, *176*, 90–101. [CrossRef] [PubMed]
14. Pu, X.X.; Ran, X.Q.; Yan, Y.; Lu, Q.Y.; Li, J.C.; Li, Y.Y.; Guan, S.P.; Cao, M.M.; Liu, J.; Hao, X.J.; et al. Three new jatrophane diterpenoids from *Euphorbia peplus* Linn. with activity towards autophagic flux. *Phytochem. Lett.* **2022**, *50*, 141–146. [CrossRef]
15. Peng, M.Y.; Zhang, X.; Li, Q.D.; Feng, E.M.; Chen, L.; Yang, H.C.; Guo, B.; Di, Y.T.; Luo, R.C.; Yan, Y.; et al. Two new jatrophane diterpenoids from *Euphorbia helioscopia* with activity towards autophagic flux. *J. Asian Nat. Prod. Res.* **2024**, *26*, 900–909. [CrossRef]
16. Jakupovic, J.; Morgenstern, T.; Bittner, M.; Silva, M. Diterpens from *Euphorbia Peplus*. *Phytochemistry* **1998**, *47*, 1601–1609. [CrossRef]
17. Shizuri, Y.; Kosemura, S.; Ohtsuka, J.; Terada, Y.; Yamamura, S. Structural and conformational studies on Euphohelioscopins A and B and related diterpenes. *Tetrahedron Lett.* **1983**, *24*, 2577–2580. [CrossRef]
18. Li, Y.; Yu, Z.P.; Li, Y.P.; Yu, J.H.; Yue, J.M. Diterpenoids from *Euphorbia peplus* possessing cytotoxic and anti-inflammatory activities. *Bioorg. Chem.* **2024**, *145*, 107194–107213. [CrossRef]
19. Corea, G.; Fattorusso, E.; Lanzotti, V.; Motti, R.; Simon, P.N.; Dumontet, C.; Di Pietro, A. Jatrophane diterpenes as modulators of multidrug resistance. Advances of structure-activity relationships and discovery of the potent lead pepluanin A. *J. Med. Chem.* **2004**, *47*, 988–992. [CrossRef]
20. Yang, Y.; Zhou, M.; Wang, D.; Liu, X.; Ye, X.; Wang, G.; Lin, T.; Sun, C.; Ding, R.; Tian, W.; et al. Jatrophane diterpenoids from Euphorbia peplus as multidrug resistance modulators with inhibitory effects on the ATR-Chk-1 Pathway. *J. Nat. Prod.* **2021**, *84*, 339–351. [CrossRef]
21. Kimura, S.; Noda, T.; Yoshimori, T. Dissection of the autophagosome maturation process by a novel reporter protein, tandem fluorescent-tagged LC3. *Autophagy* **2007**, *3*, 452–460. [CrossRef]
22. Kim, C.K.; Ahn, J.; Yu, J.; Le, D.; Han, S.; Lee, M. Analysis of antioxidant constituents from *Ilex rotunda* and evaluation of their Blood–Brain Barrier permeability. *Antioxidants* **2022**, *11*, 1989–2006. [CrossRef]